Journal of Thermal Analysis and Calorimetry, Vol. 69 (2002) 681–691

SULFONATION OF ARYLAMINES
Part 12. Kinetics of thermal decomposition of dimethylanilinium sulfates

G. Singh[1*], *I. P. S. Kapoor*[1], *J. Srivastava*[1] *and J. Kaur*[2]

[1]Chemistry Department, DDU Gorakhpur University, Gorakhpur-273009, India
[2]Materials Chemistry Division, National Chemical Laboratory, Pune, 411008, India

(Received November 15, 2001; in revised form February 8, 2002)

Abstract

Three dimethylanilinium sulfates (DMAS) have been prepared and characterised by elemental and spectral studies. Thermal decomposition of these salts have been studied by TG and simultaneous TG-DTG technique and kinetic parameters were evaluated from both dynamic and isothermal TG data using mechanism based kinetic equations. The thermal decomposition pathways have also been suggested and it has been found that DMAS salts give dimethyl aminobenzenesulfonic acids (DMABSA) via solid state reaction. The primary step in the thermal decomposition involves proton transfer followed by sulfonation.

Keywords: dimethylanilinium sulfates, DTG, TG

Introduction

The proton transfer process [1–12] has been reported to play an important role in the thermal decomposition of almost all the ammonium salts. Earlier we have prepared and characterised various mono- and disubstituted arylammonium sulphates [4–7], nitrates [8], perchlorates [9], chlorides [10], bromides [11] and fluorides [12]. The sulfate salts were found to form aminobenzenesulfonic acids during thermal decomposition, which find applications [13, 14] in organic synthesis, dyestuffs, sulfa drugs and detergents. Recently we have reported the preparation, characterisation and thermal decomposition of 2,4-; 2,5- and 3,4-dimethylanilinium sulfates [6]. In continuation to these studies, 2,6-; 3,5- and 2,3-dimethylanilinium sulfate salts (DMAS) have been prepared and their thermolysis has been reported in the present communication.

* Author for correspondence: E-mail: gsingh4us@yahoo.com

1418–2874/2002/ $ 5.00

Akadémiai Kiadó, Budapest
Kluwer Academic Publishers, Dordrecht

Table 1 Physical parameters, TLC and elemental analysis data of DMAS and DMABSA

Compound	Crystal's colour	R_f	pK_a	*m.p.*/d/ °C	Yield/ %	Elemental composition (calculated value)/%			
						C	H	N	S
(2,6-DMAS)	white, long needles	0.69 *b*:*a*=1.7:4	3.95	166	95.26	56.52 (56.47)	7.94 (7.06)	8.23 (8.24)	8.67 (9.41)
(3,5-DMAS)	white, thin flat plates	0.73 *a*:*c*=2.5:1	4.77	210 (d)	93.35	55.54 (56.47)	7.86 (7.06)	8.00 (8.24)	9.31 (9.41)
(2,3-DMAS)	white, shining amorphous	0.80 *a*:*c*=2.5:1	4.70	230 (d)	94.42	56.64 (56.47)	7.05 (7.06)	8.24 (8.24)	9.00 (9.41)
(4-A-3,5-DMBSA)	blackish green	0.76 *b*:*a*=4:3	–	>300	58.0	48.8 (47.76)	4.52 (4.52)	5.87 (5.87)	–
(4-A-2,6-DMBSA)	light brown, amorphous	0.84 *b*:*a*=4:4	–	>260	58.10	47.73 (47.76)	4.54 (4.52)	5.77 (5.87)	–
(4-A-2,3-DMBSA)	pink, amorphous	0.89 *b*:*a*=4:3	–	>300	57.90	47.41 (47.76)	4.46 (4.52)	5.83 (5.87)	–

Eluent, a (chloroform), b (acetic acid), c (methanol), locating reagent – iodine

Experimental

Materials

2,6; 3,5- and 2,3-dimethylanilines (Merck) were purified by usual method. Sulfuric acid (Merck) and silica gel TLC grade (Qualigens) were used as received.

Preparation and characterisation of DMAS

Sulfate salts were prepared by reacting corresponding amine with conc. H_2SO_4 at *RT* in 2:1 molar:

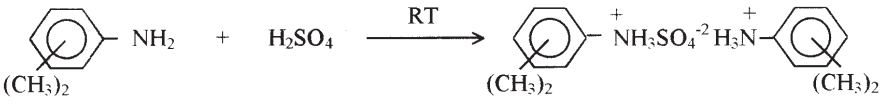

Dimethylaniline (DMA) DMAS

where $(CH_3)_2$=2,6-; 3,5- and 2,3-

Instant precipitation was obtained in all the cases and salts were washed twice with ethyl acetate to remove the unreacted amine and then recrystallized from distilled water (2,3-DMAS was recrystallized from DMF). The crystals were vacuum dried.

The purity was checked by TLC and confirmed by HPLC using DATALAB 3103 UV-VIS detector coupled with a 3101 pump and Alltech Econosil C-18 5U Column (250×4.6 mm). The purity of the compound was found to be above 98%. These salts were characterised by microanalysis, ^{1}H NMR, IR and MS spectroscopy [15–17]. Their physical parameters, details of TLC and elemental analysis data are presented in Table 1. The characteristic absorption frequencies (IR), chemical shift (1H NMR) and *m/z* values (MS) are summarised in Table 2.

Thermal decomposition of DMAS

The thermal decomposition of DMAS was investigated as follows:

Non-isothermal TG studies

TG studies on DMAS (mass 30 mg, 100–200 mesh) were undertaken in static air at heating rate of 2°C min^{-1} using indigenously fabricated TG apparatus [18] fitted with temperature-cum-controller. A round bottom gold crucible was used as sample holder. Percent decomposition (α) *vs*. temperature plots are given in Fig. 1.

Simultaneous TG/DTG studies

TG/DTG studies on DMAS (mass 10 mg, 100–200 mesh) were undertaken in N_2 atmosphere. Their plots are given in Fig. 2 and TG/DTG profile data have been summa-

Table 2 IR, ^{1}H NMR, MS data on DMAS and DMABSA

Assign.	Absorption frequency on DMAS			Assignments	Absorption frequency on DMABSA		
	2,6-DMAS	3,5-DMAS	2,3-DMAS		4-A-3,5-DMBSA	4-A-2,6-DMBSA	4-A-2,3-DMBSA
$\nu(NH_3^+)$	3400	3454	3425	$-NH_2$ sym. and asym.	3397	3454	3468
ν(C–H)	2950	3020	2900	ν(N–H)	2870	2922	2929
δ(N–H)	1600	1620	1575	δ(N–H)	1621	1605	1598
ν(C–N)	1250	1250	1260	ν(C–N)	1284	1175	1200
$\nu(SO_4^{2-})$	1100	1075	1060	$\nu(SO_3H)$	1046	1059	1040
^{1}H NMR; Chemical shift, (δ ppm)							
	6.6–7.0 (6H, aromatic)	6.5–6.9 (6H, aromatic)	6.8–7.2 (6H, aromatic)				
	2.17 (12H, Me)	4.63 (NH_3^+)	3.56 (NH_3^+)				
		2.21 (12H, Me)	1.9–2.6 (12H, Me)				
MS (relative intensity) *m/z*							
	121 (100)	121 (100)	106 (100)				
	106 (60)	106 (50)	121 (90)				
	91 (16)	91 (9)	77 (63)				
	77 (18)	77 (10)	91 (35) 60 (10) 53 (6)				

rised in Table 3. Kinetic parameters reported in Table 4 were evaluated using Coats–Redfern (CR) [19], Horowitz–Metzger [20] equations.

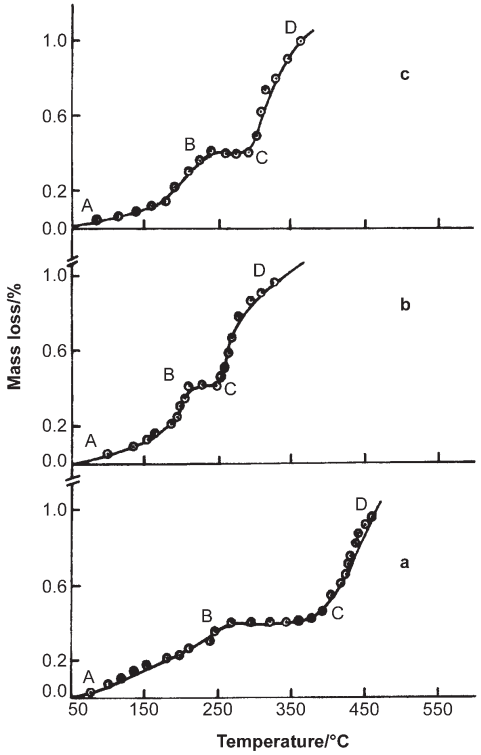

Fig. 1 TG curves of a – 2,6-DMAS; b – 3,5-DMAS; c – 2,3-DMAS; A→B: decomposition of DMAS; B→C: stability of DMABSA; C→D: decomposition of DMABSA

Table 3 TG and DTG profile data of DMAS

Compound	TG of DMAS (N_2)			Stability range of DMABSA/°C	DTG peaks temp./°C (N_2)	
	S_{dt}	F_{dt}	mass loss/%		I	II
2,6-DMAS	108	256	43.5	256–335	243	343
3,5-DMAS	126	273	43.0	273–336	257	348
2,3-DMAS	212	278	38.0	278–356	263	393

S_{dt}=starting decomposition temperature
F_{dt}=final decomposition temperature

Table 4 Kinetic parameters for non-isothermal decomposition of DMAS using CR, and HM equations

Compound	Kinetic model	Coats–Redfern Eq. (n=0)		Horowitz–Metzger Eq. (n=0)	
		E_a/kJ mol^{-1}	r	E_a/kJ mol^{-1}	r
2,6-DMAS	R_2	109.0	0.9949	131.0	0.9970
	R_3	112.0	0.9945	134.0	0.9969
3,5-DMAS	R_2	193.0	0.9950	218.0	0.9941
	R_3	195.0	0.9954	221.0	0.9944
2,3-DMAS	R_2	150.0	0.9955	169.0	0.9961
	R_3	150.0	0.9954	171.0	0.9961

Isothermal TG studies

Isothermal TG on DMAS were carried out in static air at 190±2, 205±2, 220±2, 235±2 and 250±2°C using indigenously fabricated TG apparatus. Kinetic analysis of

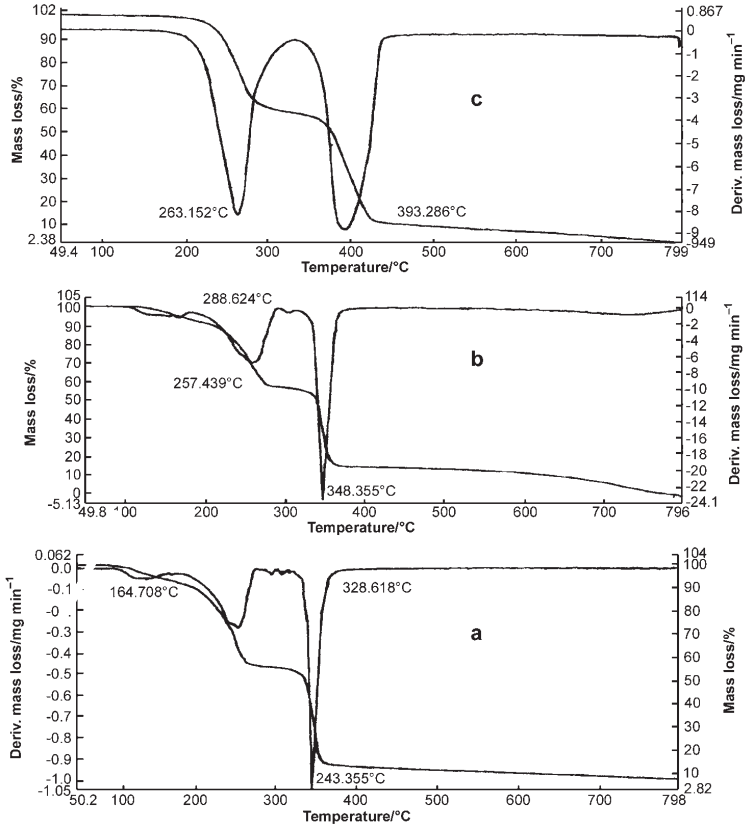

Fig. 2 Simultaneous TG/DTG curves of a – 2,6-DMAS; b – 3,5-DMAS; c – 2,3-DMAS

Table 5 Kinetic parameters and correlation coefficients (r) for isothermal decomposition of DMAS

Salt	Contracting area (n=2)							Conctracting cube (n=3)						
	Rate constant, $k\cdot10^{-2}$ /min^{-1} at T/K					r	E_a/ kJ mol^{-1}	Rate constant, $k\cdot10^{-2}$/min^{-1} at T/K					r	E_a/ kJ mol^{-1}
	463	478	493	508	523			463	478	493	508	523		
2,6-DMAS	10.7	14.0	17.5	21.0	27.0	0.9980	33.0	7.8	10.0	12.3	14.2	21.0	0.9990	35.0
3,5-DMAS	3.4	5.5	7.6	14.0	21.0	0.9878	68.0	2.5	3.8	5.5	11.5	16.0	0.9980	79.0
2,3-DMAS	2.5	5.6	9.3	12.8	18.0	0.9991	69.0	1.8	4.3	7.0	9.5	13.0	0.9961	67.0

the isothermal TG data has been made using the nine mechanism based kinetic models [21–23] and best fits were obtained in contracting area (CA) and contracting cube (CC) equations. The values of apparent activation energy (E_a), correlation coefficient (r) etc. are reported in Table 5.

Conversion of DMAS to corresponding dimethyl aminobenzenesulfonic acids (DMABSA)

The samples of 2,6-; 3,5- and 2,3-DMAS were heated respectively at 270, 210 and 220±2°C in a tube furnace [24] for 15, 50 and 40 min respectively at reduced pressure (100±2 mm Hg). Each residue was washed with ethyl acetate and dissolved in distilled water and concentrated under vacuum to get amorphous solids. Their purity was checked by TLC and HPLC. These compounds were also found to decompose during melting point determinations and were identified as 4-amino-3,5-dimethylbenzenesulfonic acid (4-A-3,5-DMBSA); 2-amino-4,6-dimethylbenzenesulfonic acid (4-A-2,6-DMBSA) and 4-amino-2,3-dimethylbenzenesulfonic acid (4-A-2,3-DMBSA). The physical parameters, details of TLC and elemental analysis data of dimethylaminobenzenesulfonic acids (DMABSA) are given in Table 1. All the DMABSA were also characterised by FTIR spectroscopy and the data are reported in Table 2. All DMABSA gave dye test and effervescence with $NaHCO_3$.

Cross sulfonation studies

The cross-sulfonation studies [5–7, 25, 26] were performed by heating each sample separately with small amount of aniline under vacuum (100±2 mm Hg) for about 30 min. The sulfanilic acid was obtained in each case alongwith the corresponding sulfonic acid (formed from salts). It indicates the formation of sulfuric acid and amine molecules in situ and sulfuric acid might have sulfonated aniline.

Results and discussion

Elemental and spectral data (Table 1) clearly indicate the formation of DMAS. TG curves show that 2,6-; 3,5- and 2,3-DMAS undergo mass loss of 43.5, 43 and 38% respectively (40.9% calculated) in the temperature range of 108–256, 126–273 and 212–278°C (Table 3, Fig. 1, A→B). The corresponding TG and DTG peak values (Fig. 2) prove the decomposition of salt to form corresponding DMABSA by the evolution of amine and water. This was also confirmed by Co-TLC and chemical analysis as reported earlier [27]. At about 100–150°C, the mass loss (Fig. 2) for 3,5- and 2,6-DMAS may be due to early evaporation of residual water from the recrystallization process. The stability of DMABSA is shown by the pleateau in TG curves (Fig. 1, (B→C), Table 3). Heating the sample beyond 335, 336 and 356°C resulted in the decomposition of corresponding DMABSA by deamination, desulfonation, dealkylation followed by ring rupture. MS data also confirm the formation of dimethylaniline cation (m/z=121) due to evolution of H_2SO_4. All DMAS when heated

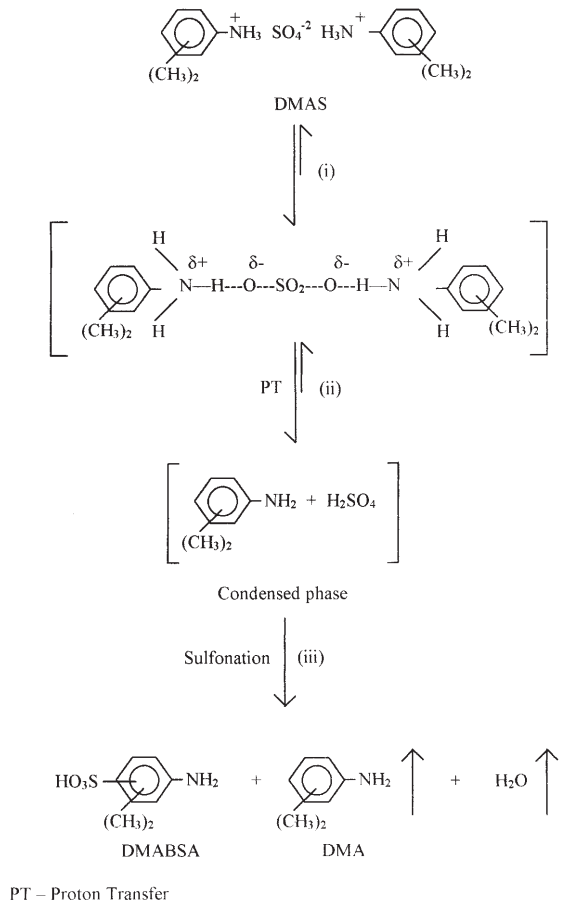

Scheme 1 Thermal decomposition pathways of DMAS

in air at higher temperature gave brownish black material containing DMABSA which was difficult to isolate. To obtain DMABSA in a pure form, samples of DMAS were heated in vacuum at a constant temperature in an indigenously fabricated tube furnace.

It has been reported [28, 29] that the basicity of the anion (SO_4^{2-}) increases with rise in temperature until it reaches the base strength of DMA. At this temperature, the anion base removes the proton from dimethylanilinium cation to form DMA and H_2SO_4 molecules. Therefore DMAS salts seem to decompose in solid state to corresponding DMA and H_2SO_4 molecule (Step 2) via proton transfer process prior to sulfonation as illustrated in Scheme 1. It is also proved by cross sulfonation studies.

Isothermal TG carried out in static air also shows mass loss for these sulfate salts and thus it was found interesting to investigate the kinetics of decomposition (Ta-

ble 5). E_a values of DMAS are lower as compared to dianilinium sulfate [30] (E_a=118 kJ mol^{-1}) which may be due to *–I* effect of CH_3 groups at *ortho* [31–33] and meta position [34–37]. Thus the N–H bond is weakened and undergo heterolysis. The low value of E_a for 2,6-DMAS seems to be due to strong *–I* effect of *ortho* CH_3 group alongwith *ortho* [33–35] and steric strain [31] whereas in 2,3- and 3,5-DMAS may be due to *ortho* strain and *–I* effect of *ortho* and *meta* CH_3 groups. A linear relationship has been found between (pK_a) [38] values of arylamine and E_a. The mechanism of thermal decomposition reaction of DMAS was also deduced from the non-isothermal TG data (Table 4) using Satava's method [21]. The striking point is that the thermal decomposition of DMAS salts is controlled by phase boundary reactions modelled by CA and CC. Although the value of E_a obtained by non-isothermal method does not match with that obtained from isothermal methods, the trend is the same.

Conclusions

Proton transfer process seems to be the primary step when sulfate salts were subjected to thermal energy and sulfonation take place forming corresponding DMABSA. The kinetic parameter for the thermal decomposition of sulfates have been found to be related to pK_a of arylamines. The rate controlling process in the thermal decomposition of DMAS seems to be phase boundary reactions modelled by CA and CC both during isothermal as well as non-isothermal heating programmes.

* * *

We are thankful to the Head of the Chemistry Department, D.D.U. Gorakhpur University for providing laboratory facilities and to NCL, PUNE for microanalysis TG/DTG, ^{1}H NMR and MS studies. UGC, New Delhi is also thanked for financial assistance.

References

1 D. G. Patil, S. R. Jain and T. B. Brill, Propellants, Pyrotech., 17 (1992) 99.
2 G. Singh, I. P. S. Kapoor, J. Singh and J. Kaur, Indian J. Chem., 39B (2000) 1.
3 T. B. Brill, P. J. Brush and T. B. Patil, Combust. Flame, 92 (1993) 178.
4 G. Singh and I. P. S. Kapoor, Indian J. Chem., 29B (1990) 57.
5 G. Singh, I. P. S. Kapoor and M. Jain, Thermochim. Acta, 292 (1997) 135.
6 G. Singh, I. P. S. Kapoor and J. Singh, Indian J. Chem., 36B (1997) 590.
7 G. Singh, I. P. S. Kapoor and J. Singh, Thermochim. Acta, 335 (1999) 11.
8 G. Singh, I. P. S. Kapoor and S. M. Mannan, Thermochim. Acta, 262 (1995) 117.
9 G. Singh, I. P. S. Kapoor and S. M. Mannan, J. Energ. Mat., 13 (1995) 141.
10 G. Singh, I. P. Kapoor and J. Kaur, Thermochim. Acta, 338 (1999) 45.
11 G. Singh, I. P. S. Kapoor and J. Kaur, J. Therm. Anal. Cal., 62 (2000) 305.
12 G. Singh, I. P. S. Kapoor and J. Kaur, Indian J. Eng. and Mat. Sci., 7 (2000) 229.
13 H. A. Lubs, The chemistry of synthetic dyes and pigments, R. E. Krieger Publ., Malabar, Florida 1982.
14 J. Bickerton, J. I. MacNeb, H. A. Skinner and G. Pilcher, Thermochim. Acta, 222 (1993) 69.

15 J. R. Dyer, Application of absorption spectroscopy of organic compounds, Prentice Hall of India Pvt Ltd., New Delhi 1987.
16 A. Ault and M. R. Ault, A handy and systematic catalog of NMR Spectra, Mill Valley, California 1980.
17 H. Gunther, NMR Spectroscopy, Wiley 1980.
18 G. Singh and R. R. Singh, Res. Ind., 23 (1978) 92.
19 A. W. Coats and J. P. Redfern, Nature, 201 (1964) 68.
20 H. H. Horowitz and G. Metzger, Anal. Chem., 35 (1963) 1464.
21 V. Satava, Thermochim. Acta, 2 (1971) 423.
22 C. M. Wyandt and D. R. Flanagon, Thermochim. Acta, 196 (1992) 379.
23 J. H. Sharp, G. W. Brindley and B. N. N. Achar, J. Am. Ceram. Soc., 49 (1966) 379.
24 G. Singh, S. K. Vasudeva and I. P. S. Kapoor, Indian J. Techn., 29 (1991) 589.
25 G. Singh, I. P. S. Kapoor and M. Jain, J. Chem. Soc. Perkin Trans. II, (1993) 1521.
26 G. Singh, I. P. S. Kapoor and M. Jain, Indian J. Chem., 35B (1996) 369.
27 J. P. Dixon, Modern methods in organic microanalysis, Van Nostrand, London 1968.
28 L. Erdey, S. Gál and G. Liptay, Talanta, 11 (1964) 913.
29 L. Erdey and S. Gál, Talanta, 10 (1963) 23.
30 G. Singh and I. P. S. Kapoor, J. Chem. Soc. Perkin Trans. II, (1989) 2155.
31 H. C. Brown and A. Cohn, J. Chem. Soc., 72 (1950) 2930.
32 G. M. Bannett and A. N. Mosses, J. Chem. Soc., (1930) 2367.
33 G. Thomson, J. Chem. Soc., (1946) 1113.
34 G. Singh and I. P. S. Kapoor, Combust. Flame, 92 (1993) 283.
35 G. Singh and I. P. S. Kapoor, J. Phys. Chem., 96 (1992) 1215.
36 P. V. R. Schlyer and G. W. Woodworth, J. Am. Chem. Soc., 90 (1963) 6530.
37 T. H. Lowry and K. S. Richardson, Mechanism and theory in organic chemistry, Harper and Row, New York 1976, p. 226 and 229.
38 J. C. Dean, Lange's Handbook of Chemistry, 13th ed., McGraw–Hill, New York 1985.